ORIGINAL ARTICLE

Journal of Research in Dental and Maxillofacial Sciences

DOI: 10.66224/jrdms.11.3. 185

Influence of Vertical Skeletal Pattern on Ramal Morphology and Optimal Screw Insertion Angulation

Sinta Elza Abraham [1], Pradeep Raj [1], Prasad Chitra [1]

[1] Department of Orthodontics and Dentofacial Orthopaedics, Army College of Dental Sciences, Secunderabad, Telangana, India, 500087.

Corresponding author:
Prasad Chitra, Department of Orthodontics and Dentofacial Orthopaedics, Army College of Dental Sciences, Secunderabad, Telangana, India, 500087

Email: prasadchitra@yahoo.co.uk

Article History
Received: 17 Dec 2025
Accepted: 20 Apr 2026

Abstract

Background and Aim: The mandibular ramus is increasingly used as an anchorage site for orthodontic miniscrews; however, anatomical variability related to vertical skeletal growth patterns may influence placement safety and stability. This study assessed mandibular ramus morphology, buccal cortical bone density, and insertion angles across different growth patterns using cone-beam computed tomography (CBCT), aiming to propose growth-pattern specific guidelines for ramal screw insertion.

Materials and Methods: This retrospective study analyzed CBCT scans of 81 adults aged 18-35 years. Subjects were equally stratified into hypodivergent, normodivergent, and hyperdivergent growth patterns. Standardized sagittal sections taken 5 mm above the occlusal plane were used to measure ramal width, thickness, height, proximity to the inferior alveolar nerve (IAN), cortical bone density, and ramal screw insertion angle. Intergroup comparisons were performed using one-way ANOVA with Tukey's post-hoc test (alpha=0.05).

Results: Vertical growth pattern significantly influenced all parameters ($P<0.001$). Hypodivergent subjects showed the greatest ramal width, thickness, and height, IAN clearance, and the highest bone density. Hyperdivergent individuals demonstrated markedly reduced dimensions and the lowest density. The modified N-angle differed significantly, being smallest in hypodivergent (8.62 degrees) and greatest in normodivergent (27.45 degrees) types.

Conclusion: The results showed that vertical skeletal growth pattern significantly influences mandibular ramal morphology, cortical bone density, and screw insertion angulation. Hypodivergent individuals exhibited the most favorable anatomical characteristics, whereas hyperdivergent individuals demonstrated reduced dimensions and density, requiring steeper insertion angulations. These findings highlight the importance of growth pattern-specific planning to enhance the safety and predictability of ramal screw placement.

Keywords: Bone Density; Bone Screws; Cone-Beam Computed Tomography; Mandibular Nerve

Cite this article as: Elza Abraham S, Raj P, Chitra P. Influence of Vertical Skeletal Pattern on Ramal Morphology and Optimal Screw Insertion Angulation. **J Res Dent Maxillofac Sci. 2026; 11(3):185-194.**

Introduction

Temporary anchorage devices (TADs) have become an essential component of contemporary orthodontics by enabling effective tooth movement without reliance on patient compliance. Among available anchorage sites, the mandibular ramus, particularly the retromolar region, has gained attention due to its dense cortical bone, making it suitable for applications such as molar distalization, uprighting, and en-masse retraction [1-3].

Compared with the buccal shelf region, the ramal site provides a more favorable posterosuperior force vector for efficient tooth movement [4]. In addition, its location away from dental roots and outside areas of active alveolar bone remodeling offers inherent anatomical safety and stability compared with interradicular regions [3]. The clinical application of ramal anchorage was further advanced by Chang et al. [3], who introduced a 14 × 2 mm OrthoBoneScrew (Newton's A Ltd., Hsinchu City, Taiwan) that provides adequate soft tissue clearance while maintaining a safe distance from the neurovascular bundle. Yeon et al. [5] demonstrated that ramal anchorage produced greater bodily distalization of the mandibular dentition with fewer unwanted effects, whereas buccal miniscrews were associated with increased molar intrusion and occlusal plane rotation. In addition, ramal screws have been shown to exhibit lower failure rates (5%) than both buccal shelf (7.2%) and interradicular miniscrews (19.5%), supporting their reliability as extra-alveolar anchorage units in complex orthodontic mechanics [3].

Despite these advantages, the success of ramal screw placement depends on accurate assessment of ramus morphology, including ramus width, height, buccolingual thickness, and the location of the inferior alveolar nerve (IAN), as inadequate evaluation may increase the risk of cortical perforation, nerve injury, or poor primary stability [2,6,7].

Earlier studies based on two-dimensional (2D) imaging reported that ramal height - measured from the most superior point of the mandibular condyle to the inferior border of the ramus - and ramal width tend to be greater in males, indicating the presence of sexual dimorphism in mandibular morphology. However, panoramic radiographs and lateral cephalograms are limited in their ability to accurately visualize the IAN or capture the true buccolingual dimensions of the ramus [8-10]. The advent of cone-beam computed tomography (CBCT) has therefore enabled three-dimensional (3D) assessment of ramal anatomy [11]. Beyond linear morphology, cortical bone density has emerged as a crucial determinant of TAD stability. Higher cortical density enhances thread engagement, resists micro-movement, and improves long-term retention. Therefore, evaluating bone density in addition to morphometric features provides a more comprehensive assessment of ramal TAD viability [1,12,13].

Patni et al. [4] proposed the N-angle, which is the angle formed between the intended ramal screw insertion path and the buccal surface of mandibular molars as a practical guide for ramal screw placement. Since ramal morphology and cortical orientation vary with vertical skeletal pattern, the optimal insertion vector may also differ. CBCT studies have shown that vertical skeletal pattern influences ramal anatomy, with hypodivergent individuals demonstrating wider rami and greater clearance from the IAN than hyperdivergent subjects [6,7]. However, existing analyses have largely focused on isolated parameters such as transverse width or thickness [6], often in small samples [7], without evaluating nerve proximity, cortical bone density, or insertion angulation together [6,7]. Similarly, although the region 3-8 mm above the occlusal plane has been identified as relatively wide and safe for screw placement, variations related to skeletal growth pattern and bone density have not been considered [14].

Importantly, cortical bone density and insertion angulation, both key factors for anchorage safety and stability, have not been assessed in a growth pattern–specific manner. Therefore, this study aimed to provide a comprehensive CBCT-based evaluation of ramal dimensions, cortical bone density, IAN proximity, and insertion angulation using the N-angle across different vertical skeletal growth patterns to support safer and more predictable ramal screw placement.

Materials and Methods

This retrospective cross-sectional study was conducted on CBCT scans of 81 individuals (30 males and 51 females) obtained from the archives of the Department of Oral Medicine and Radiology in the Army College of Dental Sciences, Secunderabad, India. Ethical approval was obtained from the institutional review board before data collection (ACDS/IEC/202/03/2024). All participants were between 18 and 35 years, had fully erupted permanent dentition, and no history of facial trauma, craniofacial anomalies, or prior surgical intervention. The required sample size was determined considering alpha=0.05, beta=0.2, and study power of 80%. Subjects were divided equally into hypodivergent (n=27), normodivergent (n=27) and hyperdivergent (n=27) facial types based on the mandibular plane angle (SN–GoGn) derived from lateral cephalograms [15-17]. SN–GoGn was selected as it is a widely accepted and reproducible parameter for assessing vertical skeletal pattern and allows comparison with previous orthodontic and CBCT-based studies [7,14]. CBCT imaging was performed using a NewTom Giano CBCT scanner (Cefla S.C., Imola, Italy) with standardized parameters: 8×10 cm field of view, 0.25 mm voxel size, 90 kVp tube voltage, and 3.6 mAs exposure time. Data were exported in DICOM format, and images were reconstructed using NNT software (NewTom, Italy). To ensure reproducibility, the Frankfort horizontal plane was oriented parallel to the floor, and the occlusal plane was standardized as the horizontal reference for all reconstructions [7,14]. Measurements were carried out on the right mandibular ramus to avoid bilateral variability. In each case, a true sagittal cross-section passing midway between the external and internal oblique ridges was selected. A single slice taken 5 mm above the occlusal plane served as the reference level for all measurements, as this region lies above the mandibular foramen and provides a safe and stable site for ramal screw insertion [6]. Linear measurements were performed using NNT's measuring tool and included ramal width (from the deepest point of the coronoid notch to the posterior border of ramus) [6], ramal thickness (from internal oblique ridge to external oblique ridge) [11], ramal height (distance from the sigmoid notch to the inferior mandibular border) [11], and the shortest distance from the anterior border of ramus to the anterior border of the mandibular canal (IAN proximity) (Figure 1).

The occlusal plane was defined by a line joining the mandibular right central incisor incisal edge and mesiobuccal cusp of the mandibular right first molar. The coronal and sagittal planes were oriented along the mesiobuccal and central groove of the mandibular right first molar [14] (Figure 2).

All measurements were recorded by one single examiner to the nearest 0.01 mm, and each parameter was measured twice. To assess intra-observer reliability, 18 CBCT scans were randomly selected, and all measurements were repeated by the same examiner after a two-day interval. The intra-class correlation coefficient was calculated using a two-way mixed-effects model with absolute agreement [18]. To evaluate ramal screw insertion angle in relation to facial divergence, a modified version of the N-angle proposed by Patni et al. [4] was incorporated into this study. In their original method, the angle was formed relative to the buccal cusp line of the mandibular molars. In the present study, the angle was measured between the ramal insertion line and a reference line drawn along the central groove of the mandibular first molar (Figure 3).

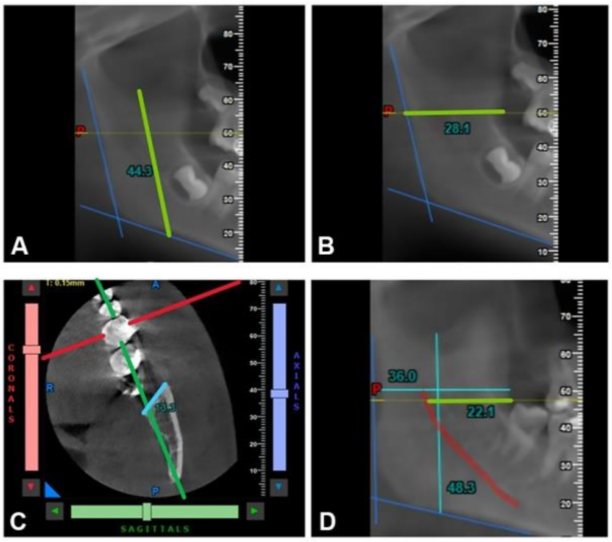

Figure 1. CBCT-based linear measurements of the mandibular ramus: (A) Ramal height, (B) ramal width, (C) ramal thickness and (D) IAN proximity

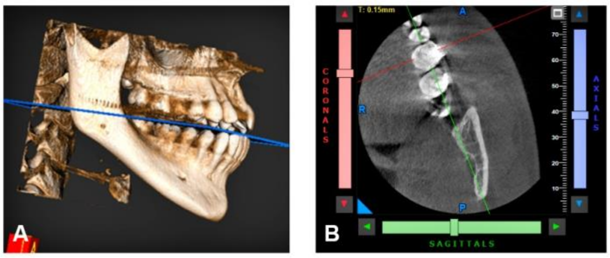

Figure 2. Reference planes: (A) Occlusal, (B) coronal (red) and sagittal (green)

This modification was necessary because the measurement slice was standardized at 5 mm above the occlusal plane, where buccal cusps were not reliably identifiable. The central groove was chosen for its consistent anatomical visibility and has been previously employed as a reference landmark in CBCT-based morphometric assessments of the mandibular ramus [7,14]. To complement linear morphometry with an evaluation of bone quality, cortical bone density was measured in Hounsfield Units (HU) using the Trace Profile tool of NNT Viewer [19]. In each selected slice, a line was drawn perpendicular to the buccal cortical plate at the designated insertion site, extending from the external surface through the cortical layer without entering the trabecular bone. The software generated a density curve along the traced line, and the maximum HU value - representing the most mineralized portion of the cortical plate - was recorded as the buccal cortical bone density for that subject. All scans were analyzed under identical machine settings and reconstruction conditions. Brightness and contrast were not altered to preserve numerical HU accuracy. Bone-quality classification provided by Resnik and Misch [20] (D1>1250 HU, D2=850–1250 HU, D3=350–850 HU, D4<350 HU) was used to aid interpretation. This protocol allowed for consistent densitometric comparison of cortical bone across different facial growth patterns.

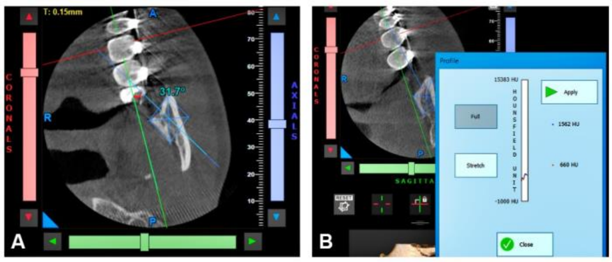

Figure 3. Evaluation of insertion angulation and cortical bone density on CBCT scans: (A) Modified N-Angle and (B) Cortical bone density using trace profile

Statistical analysis:

Data were organized in Microsoft Excel (Microsoft Corp., Redmond, WA, USA) and analyzed using IBM SPSS Statistics version 26 (IBM Corp., Armonk, NY, USA). Normality of continuous variables was assessed using the Shapiro-Wilk test, and homogeneity of variances was evaluated using Levene's test. As the assumptions for parametric testing were met, independent t-test was used to compare ramal measurements between males and females, and one-way ANOVA was applied to evaluate differences among hypodivergent, normodivergent, and hyperdivergent growth patterns. Wherever ANOVA revealed statistically significant differences, Tukey's post-hoc test was employed to control for type I error during multiple pairwise comparisons.

Relationships among ramal width, thickness, height, and IAN proximity were analyzed using Pearson's correlation test after confirming linearity and the absence of influential outliers through visual inspection of scatter plots. The Spearman's rank correlation was used to evaluate associations involving ordinal variables, including vertical skeletal growth pattern, cortical bone density, and the modified N-angle. A P value of less than 0.05 was considered statistically significant.

Results

CBCT analysis revealed significant differences in mandibular ramal morphology among hypodivergent, normodivergent, and hyperdivergent growth patterns. The intra-observer reliability was excellent for all measurements, with intra-class correlation coefficient values greater than 0.92.

Ramal morphology across vertical skeletal patterns:

Transverse ramal dimensions showed a clear association with vertical skeletal pattern, with hypodivergent individuals demonstrating the greatest ramal width and buccolingual thickness, followed sequentially by normodivergent and hyperdivergent groups. These intergroup differences were statistically significant (P=0.001, Table 1). Ramal height also varied significantly with growth pattern and was notably reduced in hyperdivergent individuals when compared with hypodivergent and normodivergent subjects (P=0.001), between whom no significant difference was observed (P=0.746, Table 1).

IAN proximity and cortical bone density:

The distance between the mandibular canal and the outer ramal cortex was the greatest in hypodivergent individuals and significantly reduced in both normodivergent and hyperdivergent groups (P=0.001), with comparable values between the latter two (P=0.320, Table 1).

Cortical bone density demonstrated a strong dependence on vertical skeletal pattern. Hypodivergent individuals exhibited the highest density values, corresponding predominantly to D1-type bone, whereas hyperdivergent subjects showed significantly lower density values consistent with D2-type bone (P=0.001). Normodivergent individuals demonstrated intermediate values (Table 2).

Table 1. Comparison of ramal morphology across hypodivergent, normodivergent, and hyperdivergent groups using one-way ANOVA and Tukey's post-hoc test

Parameter	Hypodivergent (Mean ± SD)	Normodivergent (Mean ± SD)	Hyperdivergent (Mean ± SD)	ANOVA P value	Tukey Comparison
Ramal Width (mm)	33.59 ± 1.13	31.55 ± 1.13	29.79 ± 1.07	<0.001	Hypo > Normo > Hyper
Ramal Thickness (mm)	12.31 ± 1.00	10.78 ± 0.79	9.28 ± 0.91	<0.001	Hypo > Normo > Hyper
Ramal Height (mm)	44.72 ± 1.27	44.99 ± 1.22	42.28 ± 1.55	<0.001	Hyper < Hypo = Normo
IAN Proximity (mm)	17.67 ± 1.08	12.83 ± 0.90	13.19 ± 0.70	<0.001	Hypo > Hyper > Normo

IAN: Inferior alveolar nerve; SD: Standard deviation; Hypo: Hypodivergent; Hyper: Hyperdivergent; Normo: Normodivergent

Table 2. Comparison of cortical bone density and modified N-angle among vertical growth patterns using one-way ANOVA and Tukey's post-hoc test

Parameter	Hypodivergent (Mean ± SD)	Normodivergent (Mean ± SD)	Hyperdivergent (Mean ± SD)	ANOVA P value	Tukey Comparison
Cortical Bone Density (HU)	1592.38 ± 177.69	1465.23 ± 134.45	1147.28 ± 135.67	<0.000	Hypo > Normo > Hyper
Modified N-Angle (degrees)	8.61 ± 2.06	27.44 ± 2.02	21.72 ± 1.97	<0.001	Normo > Hyper > Hypo

HU: Hounsfield Unit; SD: Standard deviation; Hypo: Hypodivergent; Hyper: Hyperdivergent; Normo: Normodivergent

Ramal screw insertion angulation:

The modified N-angle also differed significantly across growth patterns (P=0.001). Hypodivergent subjects showed the smallest angulation values, normodivergent individuals demonstrated the greatest angulation, and hyperdivergent subjects exhibited intermediate values, with all pairwise comparisons reaching statistical significance (P<0.05, Table 2).

Post-hoc and correlation analyses:

Post-hoc analysis confirmed significant pairwise differences among all three growth-pattern groups for ramal dimensions, cortical bone density, and modified N-angle measurements (P<0.05). Correlation analysis further revealed a strong inverse relationship between vertical growth pattern and cortical bone density (r=−0.773, P=0.000), indicating a progressive reduction in density from hypodivergent to hyperdivergent patterns. In contrast, a moderate positive correlation (r=0.481, P=0.000) was observed between growth pattern and modified N-angle, suggesting that steeper insertion angulations were associated with more vertical skeletal patterns.

Sex-based differences in ramal morphology:

Sex-based comparisons demonstrated significant sexual dimorphism in transverse ramal dimensions, with males exhibiting greater ramal width and thickness than females (P=0.001 and P=0.002, respectively). However, no significant sex-related differences were observed for ramal height or proximity to the IAN (P>0.05).

Discussion

The present 3D study demonstrated that vertical skeletal growth pattern had a strong influence on mandibular ramal morphology, cortical bone characteristics, IAN proximity, and optimal screw insertion angulation. These differences are not isolated findings but reflect underlying variations in mandibular growth direction, functional loading, and bone remodeling associated with different facial types.

Ramal width was the greatest in hypodivergent individuals and progressively reduced in normodivergent and hyperdivergent subjects. This can be explained by the forward rotational growth pattern typically seen in low-angle faces, which promotes bone apposition along the posterior border of the ramus, whereas backward rotators exhibit limited transverse growth [21]. Recent CBCT evidence further supports this observation, reporting significantly narrower rami in hyperdivergent individuals compared with hypodivergent subjects [15]. Rathor et al. [7] similarly documented wider rami in low-angle cases.

Ramal height was significantly greater in hypodivergent and normodivergent individuals than in hyperdivergent subjects. This finding reflects differences in posterior facial height development related to mandibular rotation. Schudy [22] described that low-angle individuals exhibit enhanced posterior vertical growth due to forward mandibular rotation, whereas high-angle individuals show reduced posterior facial height due to backward mandibular rotation.

The greater ramal height observed in hypodivergent individuals in the present study is consistent with recent CBCT evidence demonstrating significantly reduced ramus height in hyperdivergent subjects, reflecting limited posterior vertical development in high-angle facial patterns [15,23].

Ramal thickness, measured from the internal oblique ridge to the external oblique ridge, was the greatest in hypodivergent individuals and least in hyperdivergent subjects. Unlike ramal height and width, ramal thickness appears to be strongly influenced by functional loading. Simonek et al. [24] demonstrated that increased masticatory muscle activity and higher bite forces stimulate periosteal bone apposition and increase bone mass, whereas reduced muscle function results in thinner mandibular structures. Hypodivergent individuals generally generate greater masticatory forces, leading to adaptive thickening of the ramus, while hyperdivergent individuals exhibit lower functional loading and reduced strain, resulting in diminished ramal thickness. Recent CBCT studies have similarly reported reduced ramal thickness in hyperdivergent subjects compared with hypodivergent individuals, supporting the role of growth pattern-dependent functional adaptation in determining ramal thickness [6,7]. From a clinical standpoint, thicker and taller rami offer improved mechanical interlocking and wider safety margins, allowing placement of longer or wider miniscrews with more predictable primary stability and a reduced risk of cortical perforation or nerve injury.

The distance between the IAN and the outer ramal cortex was the greatest in hypodivergent individuals and significantly reduced in hyperdivergent subjects. This difference is largely a consequence of reduced ramal width in high-angle faces. CBCT studies similarly reported decreased nerve clearance in hyperdivergent individuals, increasing the risk of nerve proximity during ramal screw placement [6,7,15]. Clinically, this reduced safety margin necessitates more cautious planning and modified insertion angulation.

Cortical bone density also showed a clear dependence on vertical skeletal pattern. Hypodivergent individuals demonstrated higher density values in D1-type bone, whereas hyperdivergent individuals exhibited lower-density D2-type bone. This variation is most likely related to differences in functional loading and muscle-induced bone remodeling. Individuals with stronger masticatory muscles and lower mandibular plane angles experience greater functional strain, which promotes cortical mineralization and increased bone density, whereas reduced functional demand is associated with lower-density bone [24,25].

These observations are consistent with previous studies reporting denser mandibular cortices in brachyfacial individuals compared with dolichofacial types [25]. Furthermore, Vargas et al. [26] and Azeem et al. [27] demonstrated that increased mandibular plane angles are associated with reduced cortical density and lower success rates of TADs.

Clinically, while higher cortical density enhances screw retention, it also increases insertion torque, potentially leading to heat generation, microdamage, or screw fracture. In such situations, slow-speed self-drilling or predrilling techniques may help mitigate these risks [28]. Conversely, the lower cortical density observed in hyperdivergent individuals, although easier to penetrate, may compromise mechanical stability, highlighting the need for careful case selection, modified screw dimensions, or delayed loading protocols. The findings of Zhao et al. [29] further support these observations. Their analysis of retromolar space demonstrated that hyperdivergent individuals possess reduced posterior mandibular volume, narrower ramal width, and limited distalization space - features that indirectly reflect reduced cortical bone availability. Although their study did not specifically address TAD placement, it reinforces the broader anatomical constraints associated with vertical growth patterns.

Evaluation of the modified N-angle revealed significant variation across growth patterns. Hyperdivergent patients required a steeper insertion angle (approximately 21 degrees) to maximize bone engagement while maintaining a safe distance from the mandibular canal, consistent with the observations of Yeon et al. [5]. Normodivergent individuals demonstrated the highest mean angulation (approximately 27 degrees), whereas hypodivergent subjects required a relatively flatter insertion path due to their broader and more horizontally oriented ramal surfaces. This geometric requirement is further influenced by the propeller-like curvature of the ramus and reduced posterior mandibular volume in high-angle cases [4]. Clinically, these findings emphasize that insertion angulation should be individualized not only to avoid the IAN but also to accommodate local osseous contours, with flatter angulation preferred in low-angle cases and steeper angulations required in high-angle individuals.

Sex-based differences were also evident, with males demonstrating greater transverse ramal width and thickness. These differences are likely influenced by hormonal and functional factors, including increased masticatory muscle activity and prolonged skeletal maturation in males [30,31]. Clinically, this suggests that male patients may better accommodate longer or larger-diameter miniscrews and tolerate higher insertion torque without compromising stability. In contrast, female patients, particularly those with hyperdivergent growth patterns, may require more conservative screw selection and insertion strategies to minimize the risk of cortical perforation or inadequate primary stability.

Taken together, these findings reinforce the importance of individualized assessment of ramal morphology when planning orthodontic anchorage. Comparative evaluation across studies highlights vertical facial divergence as a key determinant of ramal anatomy, influencing the feasibility, location, and angulation of screw placement. Future research should aim to include larger and more diverse populations to better capture ethnic and anatomical variability. Prospective clinical studies evaluating ramal screw stability and complication rates using growth pattern-specific protocols would further validate the recommendations proposed here. In addition, finite element analyses could provide valuable insight into stress distribution around screws placed at varying angulations, particularly in hyperdivergent patients with reduced cortical density. Consideration of soft tissue thickness and the use of CBCT-guided surgical templates may further enhance precision, safety, and long-term predictability of ramal screw placement.

This investigation was limited to an Indian adult population, which may restrict the generalizability of the findings to other ethnic groups with differing craniofacial characteristics. As this was a single-center, retrospective study, the findings should be interpreted with caution, and extrapolation to other populations or ethnic groups may be limited. Measurements were obtained from a standardized sagittal slice 5 mm above the occlusal plane, which may not fully capture the 3D variability of the ramus. In addition, clinical outcomes such as actual screw stability were not assessed, underscoring the need for future prospective clinical studies.

Conclusion

Hypodivergent individuals exhibited the most favorable anatomical conditions, characterized by wider and thicker rami, higher cortical density, greater IAN clearance, and flatter insertion angle that support high primary stability. In contrast, normodivergent and hyperdivergent individuals demonstrated an increased modified N-angle, suggesting that optimal screw angulation in this group may require a more oblique insertion.

Funding

None

Conflict of Interest

None

References

1. Wang S, Bing L, Park HS. Optimal microimplant sites in the mandibular retromolar area: Mesh analysis of cortical bone thickness and density in CBCT images. Int. J. Morphol. 2021;39(3):907-14.

2. Chang CH, Lin JS, Roberts WE. Ramus screws: the ultimate solution for lower impacted molars. Semin Orthod. 2018 Mar;24(1):135–54.

3. Chang C, Lin SY, Roberts WE. Forty consecutive ramus bone screws used to correcthorizontally impacted mandibular molars. Int J Orthod Implantol. 2016 Jan;41:60–9.

4. Patni VJ, Kolge NE, Pednekar MJ. N-Angle: Clinical indicator for predictable insertion of ramal bone screws. J Indian Orthod Soc. 2021 Oct;55(4):384-9.

5. Yeon BM, Lee NK, Park JH, Kim JM, Kim SH, Kook YA. Comparison of treatment effects after total mandibular arch distalization with miniscrews vs ramal plates in patients with Class III malocclusion. Am J Orthod Dentofac Orthop. 2022 Apr;161(4):529-36.

6. Mehta S, Arqub SA, Sharma R, Patel N, Tadinada A, Upadhyay M, et al. Variability associated with mandibular ramus area thickness and depth in subjects with different growth patterns, gender, and growth status. Am J Orthod Dentofac Orthop. 2022 Mar;161(3):e223–34.

7. Rathor A, Shah A, Jani B, Vekariya J, Shah VM. Comparative evaluation of bone anatomy for ramal implant placement and proximity to the inferior alveolar canal in different facial divergence to assess the ideal site of placement: a cone-beam computed tomography study. Cureus. 2025 Jan;17(1):e78290.

8. Mehta H, Bhuvaneshwari S, Singh MP, Nahar P, Mehta K, Sharma T. Gender determination using mandibular ramus and gonial angle on OPG. J Indian Acad Oral Med Radiol. 2020;32(2):154-8.

9. Koju S, Maharjan N, Rajak RRK, Yadav DK, Bajracharya D, Ojha B. Assessment of sexual dimorphism in mandibular ramus: an orthopanoramic study. Kathmandu Univ Med J. 2021 Sep;19(3):314–9.

10. More CB, Vijayvargiya R, Saha N. Morphometric analysis of mandibular ramus for sex determination on digital orthopantomogram. J Forensic Dent Sci. 2017 Jan;9(1):1-5.

11. Kronseder K, Runte C, Kleinheinz J, Jung S, Dirksen D. Distribution of bone thickness in the human mandibular ramus – a CBCT-based study. Head Face Med. 2020 Jun;16(1):13.

12. Hasani M, Afzoon S, Karandish M, Parastar M. Three-dimensional evaluation of the cortical and cancellous bone density and thickness for miniscrew insertion: a CBCT study of interradicular area of adults with different facial growth pattern. BMC Oral Health. 2023;23(1):753.

13. Pan CY, Liu PH, Tseng YC, Chou ST, Wu CY, Chang HP. Effects of cortical bone thickness and trabecular bone density on primary stability of orthodontic mini-implants. Journal of dental sciences. 2019;14(4):383-8.

14. Maliael MT, George AM, Aravind TRP, Chellappa LR, Varghese RM. Quantitative assessment of ramal bone width and the proximity of the inferior canal for the predictable insertion of ramal implants: cone-beam computed tomography study. APOS Trends Orthod. 2023 Mar;13(3):146–52.

15. Rajesh R, Gupta S, Chakraborty S, Patil SS, Chauhan A, Mukherjee A, Chakraborty SC. Three-dimensional assessment of mandibular morphology across vertical facial growth patterns using cone-beam computed tomography: a cross-sectional study. Cureus. 2025 May;17(5).

16. Trivedi K, Jani BK, Hirani S, Radia MV. Comparative evaluation of cortical bone anatomy of mandibular buccal shelf for mini implant placement in different facial divergence: a cone beam computed tomography study. J Indian Orthod Soc. 2020 Oct;54(4):325-31.

17. Feng X, Weng L, Li X, Shen Y, Lin J. Optimal sites for miniscrew insertion in anterior aesthetic region: a CBCT study for different vertical skeletal patterns. BMC Oral Health. 2025 Jul;25(1):1148.

18. Koo TK, Li MY. A guideline of selecting and reporting intraclass correlation coefficients for reliability research. J Chiropr Med. 2016 Jun;15(2):155-63.

19. Rai S, Misra D, Misra A, Tomar H, Dhawan A, Gupta R. Reliability of Grayscale Value for Bone Density Determination in Oral Rehabilitation using Dental Implants. Int J Appl Basic Med Res. 2023 Jul;13(3):143–8.

20. Resnik RR, Misch CE. Bone density: A key determinant for treatment planning. In: Misch's Contemporary Implant Dentistry. 4th ed. St. Louis: Elsevier; 2020. Chapter 18, pp. 450–65.

21. Björk A, Skieller V. Facial development and tooth eruption. An implant study at the age of puberty. Am J Orthod. 1972 Oct;62(4):339-83.

22. Schudy FF. Vertical growth versus anteroposterior growth as related to function and treatment. Angle Orthod. 1964 Apr;34(2):75-93.

23. Lemes CR, Tozzi CF, Gribel S, Gribel BF, Venezian GC, do Carmo Menezes C, Custodio W. Mandibular ramus height and condyle distance asymmetries in individuals with different facial growth patterns: a cone-beam computed tomography study. Surg Radiol Anat. 2021 Feb;43(2):267-74.

24. Simonek M, Türp JC, Bornstein MM, Dagassan-Berndt D. Prevalence and correlation with sex, age, and dental status of bone apposition at the mandibular angle and radiographic alterations of the temporomandibular joints: a retrospective observational study in an adult Swiss population. BMC Oral Health. 2024 Feb;24(1):193.

25. Teterina A, Niratisairak S, Morseth B, Bolstad N. General and local predictors of mandibular cortical bone morphology in adult females and males: the seventh survey of the Tromsø Study. Clin Oral Investig. 2023 Nov;27(11):6577-87.

26. Vargas EO, de Lima RL, Nojima LI. Mandibular buccal shelf and infrazygomatic crest thicknesses in patients with different vertical facial heights. Am J Orthod Dentofacial Orthop. 2020 Sep;158(3):349-56.

27. Azeem M, Saleem MM, Liaquat A, Haq AU, Hamid WU, Masood M. Failure rates of mini-implants inserted in the retromolar area. Int Orthod. 2019 Mar;17(1):53-9.

28. Fang X, Ding H, Fan C, Pang L, Xu T, Liu J, et al. Comparison of mandibular buccal shelf morphology between adolescents and adults with different vertical patterns using CBCT. Oral Radiol. 2024 Jan;40(1):58-68.

29. Zhao Z, Wang Q, Yi P, Huang F, Zhou X, Gao Q, et al. Quantitative evaluation of retromolar space in adults with different vertical facial types. Angle Orthod. 2020 Nov;90(6):857–65.

30. Meleveetil DB, Beena VT, Cheriyan LM, Angamuthu K, Charapparambath B. Mandibular ramus: an indicator of gender and chronological Age-A digital radiographic study. J Forensic Dent Sci. 2020 Sep;12(3):158-64.

31. Astuti ER, Iskandar HB, Nasutianto H, Pramatika B, Saputra D, Putra RH. Radiomorphometric of the jaw for gender prediction: a digital panoramic study. Acta Med Philipp. 2021;55(2):113-21.